

Quantum-Enhanced Interferometer for Multiphase Sensing

Yanni Feng,^{1,*} Zhaoqing Zeng,^{1,*} Jialin Cheng,^{1,*} Zhaolin You,¹ Huadong Lu,^{1,2,†} Zhihui Yan,^{1,2,‡} Xiaojun Jia,^{1,2,§} Changde Xie,^{1,2} and Kunchi Peng^{1,2}

¹*State Key Laboratory of Quantum Optics Technologies and Devices, Institute of Opto-Electronics, Shanxi University, Taiyuan 030006, People's Republic of China*

²*Collaborative Innovation Center of Extreme Optics, Shanxi University, Taiyuan 030006, People's Republic of China*

 (Received 16 November 2024; revised 19 September 2025; accepted 7 October 2025; published 28 October 2025)

Quantum-enhanced interferometers have been widely used in single-parameter precision measurement, and multiparameter precision measurement is the building block of numerous sensing and imaging applications. However, it remains challenging to realize high-sensitivity multiparameter sensing without increasing power, which is crucial for biological science. Here, we propose and demonstrate a deterministic quantum-enhanced interferometer, where high-sensitivity multiparameter sensing is realized by effectively squeezing noises and amplifying signals. Key technologies are essential to the results, including the parallel and sequential use of squeezed states inside the interferometer. Notably, in the quantum-enhanced three-arm interferometer, not only joint but also individual values of three signals are simultaneously measured with a signal-to-noise ratio of more than 10.37 ± 0.13 dB compared with that of the conventional interferometer under the same phase-sensing power. These advances constitute a critical step toward observing multiple elusive signals and give rise to a wide range of sensing and imaging applications.

DOI: [10.1103/PhysRevLett.135.183602](https://doi.org/10.1103/PhysRevLett.135.183602)

Interferometers have been exploited in ultrasensitive measurements of phase-related observables [1]. Substantial progress in the development of interferometers has led to a plethora of groundbreaking applications, such as observations of gravitational waves [2]. With the development of optical interferometers, the multiarm interferometer consists of multiple spatially separated optical beams as the arms of interferometer [3], and is key for many practical applications [4]. The combination of an array of single-mode squeezed states and a multiarm interferometer enables a large mode number to route and process multiple optical modes for complex applications, such as Gaussian boson sampling [5,6]. The multiarm interferometer can collectively undertake multiparameter precision measurement tasks. The multiarm interferometer can simultaneously measure multiple phase-related weak signals for potential applications through parallel architecture, ranging from multichannel optofluidic devices [7,8] to high-speed photoacoustic sensors [9]. Therefore, the high-sensitivity interferometer holds promise for applications in multiparameter precision measurement.

The sensitivity of the interferometer can be dramatically improved by increasing the phase-sensing power. However, high power severely disturbs the function, structure, and

growth of living systems, and it is impossible to improve sensitivity by increasing the power used in biological sensing [10]. Thus, the performance of an interferometer is ultimately limited by the inherent noise associated with the shot noise limit (SNL), owing to photon number fluctuations in the electromagnetic field [11,12]. Quantum-enhanced precision measurements exploit quantum resources to increase sensitivity beyond the SNL [13], and have great potential for both fundamental science and concrete applications [14–16]. Great efforts have been devoted to quantum-enhanced interferometers [17–20], where the squeezed state enables a 3 dB sensitivity improvement in gravitational wave detection [21,22]. Furthermore, the capabilities of multiparameter sensing can be empowered by using quantum technology [23–29]. The rich achievements of distributed quantum sensing in a network [30–33] have been demonstrated, and the detection of a linear combination of distributed phases beyond the SNL is achieved in a truncated SU(1,1) interferometer [34]. Yet a critical problem for biosensing today is realizing high sensitivity for multiparameter detection without increasing the power to avoid the photodamage limit. Moreover, while joint sensing among different modes can evaluate the concentration of analytes in a given area, the individual signals provide information about local information. So far, it is a longstanding goal to improve the multiparameter sensitivity through quantum technology; however, it is a key remaining challenge to achieve the high sensitivity, and scalable and robust multiphase measurements without increasing power. Furthermore, not only joint but also

*These authors contributed equally to this work.

†Contact author: luhuadong@sxu.edu.cn

‡Contact author: zhyan@sxu.edu.cn

§Contact author: jjaxj@sxu.edu.cn

individual measurements of multiple elusive signals beyond classical limits are required for much insight into complex processes, due to the difficulty in effectively using quantum states, jointly processing multiple parameters, and complex configurations.

Here we demonstrate high-sensitivity multiparameter sensing in a quantum-enhanced multiarm interferometer. These advances are attributed to key technologies for parallel and sequential use of squeezed states inside the interferometer. Besides multiparticle entanglement [35–37], the squeezed state provides an effective quantum resource to surpass SNL [38–41]. The high-sensitivity quantum sensing requires not only squeezing the quantum noise [42] but also amplifying the signal [43]. On the one hand, the squeezed states are directly generated inside the interferometer and, in parallel, used as phase-sensing quantum states to reduce quantum noises. On the other hand, the sequential interaction between the probe and sample can obviously amplify the signal strength. In this way, the noises are squeezed and the signals are amplified simultaneously by making full use of the squeezed states. In particular, both the joint and individual measurements of multiple phases are achieved beyond the classical limit, because of the parallel use of squeezed states. Furthermore, this quantum-enhanced interferometer allows one to gain robust and scalable multiparameter quantum sensing. The quantum advantage of this multiparameter sensing survives in a broad range of mode numbers and sample losses of the interferometer.

To experimentally demonstrate the quantum superiority of three-parameter sensing, a quantum-enhanced three-arm

interferometer is constructed, where three optical parametric amplifiers (OPAs) are directly coupled inside three arms of the interferometer to eliminate coupling losses. The optimal squeezing of 5.90 ± 0.10 dB is used as the original quantum source around 2 MHz, which can be widely applied in medical ultrasonic imaging [44]. The conventional interferometer stands for the classical multiarm interferometer with single-pass interaction between coherent states and samples. On the basis of the balanced homodyne detection (BHD) results, quantum noise floors of 4.68 ± 0.16 dB are squeezed below the conventional interferometer; meanwhile, the phase signals are amplified via five-pass interactions. Both the joint and individual values of the three signals are obtained simultaneously, with a signal-to-noise ratio improvement (SNRI) of 10.37 ± 0.13 dB compared with that of the conventional interferometer. Moreover, the interference destructive modes are used to avoid the saturation of photodiodes so that the high phase-sensing power is allowed. Thus, the high-sensitivity measurements of both joint and individual signals beyond classical limits are simultaneously realized without increasing power, which break the tradeoff between sensitivity and power.

A schematic diagram of the quantum-enhanced multiarm interferometer is shown in the insert of Fig. 1. The quantum-enhanced interferometer starts with a coherent state followed by the first unitary matrix U_1 based on a beam splitter array, multiple single-mode squeezed states, phase accumulations with interaction number of K , the second unitary matrix U_2 based on a beam splitter array,

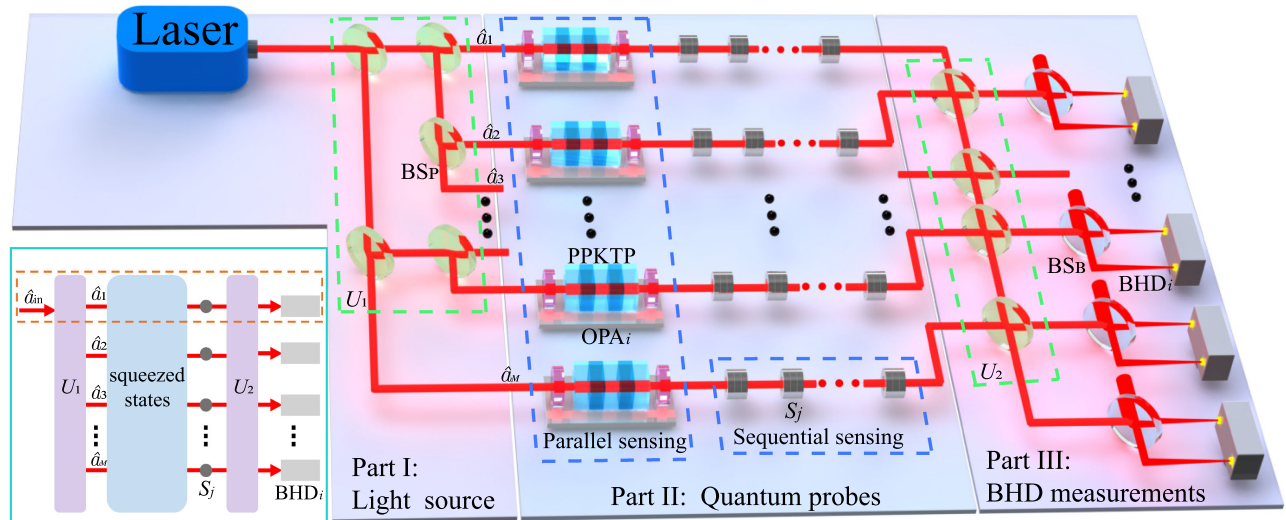


FIG. 1. Layout of a quantum-enhanced sensing of multiple phases. Part I includes light source for implementing U_1 transformation. Part II is parallel and sequential sensing with quantum probes of squeezed states, which corresponds to phase sensing with M squeezed states and K -pass interaction. Part III consists of U_2 and BHD measurements. PPKTP, periodically poled KTiOPO_4 ; OPA _{i} ($i = 1, \dots, M$), optical parametric amplifier; S_j ($j = 1, \dots, K$), phase sensor; BS_p, beam splitter with partial transmissivity; BS_B, balanced beam splitter with a transmissivity of 50%; BHD _{i} ($i = 1, \dots, M$), balanced homodyne detection. The insert is the corresponding schematic diagram, which includes a single-mode coherent state, a first unitary matrix U_1 , multiple squeezed states, phase sensing, a second unitary matrix U_2 and BHDs.

and BHDs. The unitary matrix U_1 generates probes for parallel sensing, and meanwhile interaction with K times enables sequential sensing. The unitary matrix U_2 recombines the optical modes carrying the phase signals for interference and measurement to obtain the phase changes. The quantum-enhanced interferometer can be used in multiphase sensing.

The performance of the interferometer is quantified by the sensitivity. The sensitivity can be defined as the standard deviation of the phase quadrature by error propagation, as [45] $\Delta\phi = \sqrt{\langle\Delta^2\hat{P}\rangle}/|\partial\langle\hat{P}\rangle/\partial\varphi|$, where the $\langle\Delta^2\hat{P}\rangle = \langle\hat{P}^2\rangle - \langle\hat{P}\rangle^2$ is the variance of the probe and the $\partial\langle\hat{P}\rangle/\partial\varphi$ is the rate of change with respect to a phase. The joint sensitivity of multiple phases in a quantum-enhanced interferometer is expressed as follows:

$$\Delta\phi_{J(M)} = \sqrt{\frac{(G-g)^2}{4Mk(|\alpha_{\text{PS}}|^2 - g^2)}}, \quad (1)$$

where G is the amplitude gain of the OPA ($|g|^2 = |G|^2 - 1$), α_{PS} is the phase-sensing field amplitude, the interferometric mode number M should take the integer, and k is the multipass factor. It is clear that the squeezing level, mode number, multipass interaction number, and phase-sensing power contribute to the sensitivity collaboratively. (See the Supplemental Material [46] for the sensitivity calculation details.)

The sensitivity of quantum sensing for the multiparameter under the experimental conditions is shown in Fig. 2(a). The M -arm interferometer consists of multiple optical modes with mode number M as the arms of the interferometer. The squeezed states are directly generated from OPAs inside the interferometer, which effectively use quantum states. The result shows that the higher phase sensing power and larger mode number enable higher

sensitivity, and the joint measurement of M signals with high sensitivity can be achieved in this interferometer. In this quantum-enhanced interferometer, not only can M phase changes for whole information be simultaneously measured, but the sensitivity is also enhanced by a factor of \sqrt{M} compared with the quantum-enhanced single-arm interferometer. Furthermore, the robustness and scalability are key to practical applications. The dependence of SNRI on the internal loss of the interferometer and OPA gain is analyzed in Fig. 2(b). When the OPA gain is large, the extra noise in the antisqueezing quadrature will degrade the SNRI. It is necessary to place the sample inside the arm of the interferometer, where the sample will introduce the unavoidable loss. The SNRI of multiparameter sensing is maintained with moderate OPA gain. Thus, the robust quantum-enhanced interferometer can be constructed. The function of joint sensitivity of the quantum-enhanced interferometer with respect to the mode number is demonstrated in Fig. 2(c). It can be seen that the sensitivity of the interferometer with five-pass interactions is enhanced compared with that with single-pass interaction, and the sensitivity of the interferometer can surpass that of the conventional interferometer in a broad range of mode numbers. The quantum superiority of multiparameter sensing remains to be kept with a large mode number, and it is possible to construct a scalable quantum-enhanced interferometer. These results demonstrate that the quantum-enhanced interferometer enables a high-sensitivity, robust, and scalable multiparameter sensing.

Next, a quantum-enhanced multiarm interferometer in Fig. 1 is experimentally constructed to demonstrate multiparameter quantum superiority. Part I includes a light source for implementing U_1 transformation. The coherent state laser is divided into multiple optical modes \hat{a}_i ($i = 1, \dots, M$) with equal power by the array of beam splitters and used as the inputs of the OPAs. Part II is

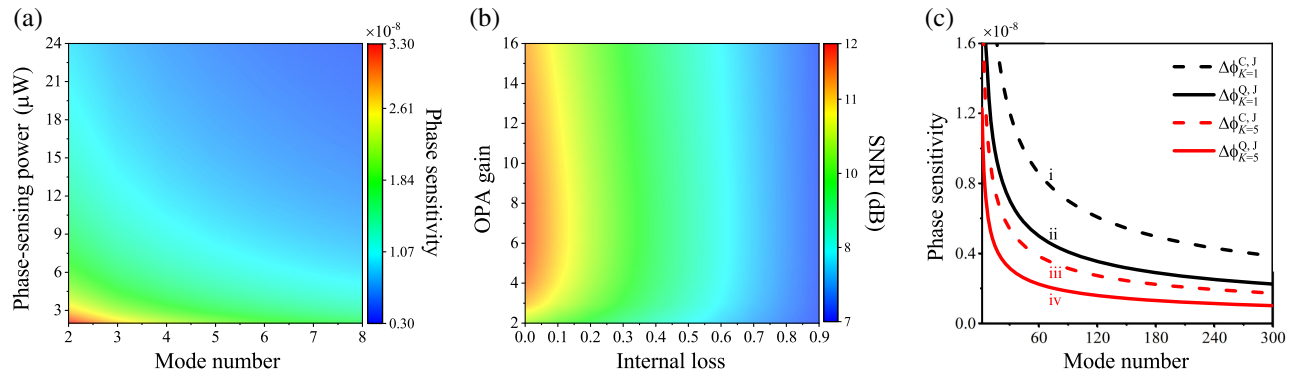


FIG. 2. The performance of quantum-enhanced interferometer. (a) Joint sensitivity vs interferometer mode number and the phase-sensing power for three signals. In the experiment, the phase fluctuation is $\theta = 0.06$ rad, the OPA intracavity loss is $\rho = 0.005$, and the total efficiency of the interferometer is $\eta_i = 0.83$. (b) The dependence of SNRI of the quantum interferometer compared with that of the conventional interferometer on the internal loss of the interferometer and OPA gain. (c) The function of joint sensitivity of the interferometer with respect to the mode number. The black (red) dashed and solid traces i (iii), ii (iv) represent the sensitivities for the classical and quantum-enhanced interferometer with single (five)-pass interaction, respectively.

parallel and sequential sensing using squeezed states. PPKTP is used as a nonlinear crystal of OPA for the generation of a squeezed state with the advantage of low loss and moderate nonlinear interaction. Squeezed states are directly generated by OPAs inside the interferometer, and effectively act as phase-sensing states to measure multiple phase changes in parallel. Notably, the sequential interaction is developed in the arms of the interferometer, where each quantum probe interacts with the sample K times to implement multipass interaction, which can effectively amplify the signal. Part III consists of U_2 and BHD measurements. All the sensor output modes are recombined by another array of beam splitters, and then the combined modes are detected to realize the joint measurements [66]. The recombination plays the role of the global measurement, where the joint sensitivity can be enhanced by the role of multiple optical modes. The combined output modes are detected by BHDs to realize the joint measurement of multiple phases, where the number of BHDs correspond to the number of sensors for individual measurements. Furthermore, the individual measurements for three (two) signals can be obtained by performing the third unitary matrix U_3 (U'_3) of the BHD measurement results. (See the Supplemental Material [46] for the sensitivity calculation details.)

To demonstrate the effect of the sequential interaction in the quantum-enhanced three-arm interferometer, Fig. 3(a) shows the influence of the interaction number on the joint sensitivity for two signals with lossy mirrors for multiple interactions. The sequential interactions can significantly enhance the sensitivity, where the phase-sensing quantum states and samples interact multiple times between two near-perfect mirrors in the experiment. Although vacuum noise is introduced to degrade the sensitivity, the sensitivity

still can be improved with lossy mirrors when the interaction number increases. The limit of SNRI is 34 dB when this interferometer loss for multiple interactions is 10^{-4} . Therefore, when the number of interactions exceeds 35, the SNRI in this interferometer can reach 20 dB. Figures 3(b) and 3(c) show the sensitivity for three and two signals in the quantum-enhanced three-arm interferometer. We can see that the five-pass interactions can improve the sensitivity because of the amplification phase signals, and the sensitivity is improved by increasing the phase-sensing power. In the quantum-enhanced sensing, the joint measurements of three phase changes require three nonlinear resources of OPAs in the arms to directly generate three bright single-mode squeezed states of 5.90 ± 0.10 dB. In each arm, the OPA output mode with $15 \mu\text{W}$ is used as a quantum probe for sensing three signals, and the corresponding photon number is $6.8 \times 10^{13}/\text{s}$. Meanwhile, the five-pass interaction between the squeezed state and sample is employed. In this three-arm interferometer, the parallel and sequential employment of squeezed states can enhance the sensitivity without increasing optical power, thereby achieving a SNRI of 10.37 ± 0.13 dB compared with the conventional interferometer, due to the signal amplification of 5.69 ± 0.15 dB and the quantum noise suppression of 4.68 ± 0.16 dB below a conventional interferometer. The quantum enhancement factor is characterized by the sensitivity of the quantum-enhanced interferometer over the corresponding SNL for fixed resources [67]. The quantum enhancement factors of 3.5 and 1.6 are achieved with single- and five-pass interactions, respectively. (See the Supplemental Material [46] for the performance of the quantum-enhanced interferometer details.) Furthermore, a higher sensitivity for two signals is achieved than that of three signals. The higher sensitivity can be obtained for two

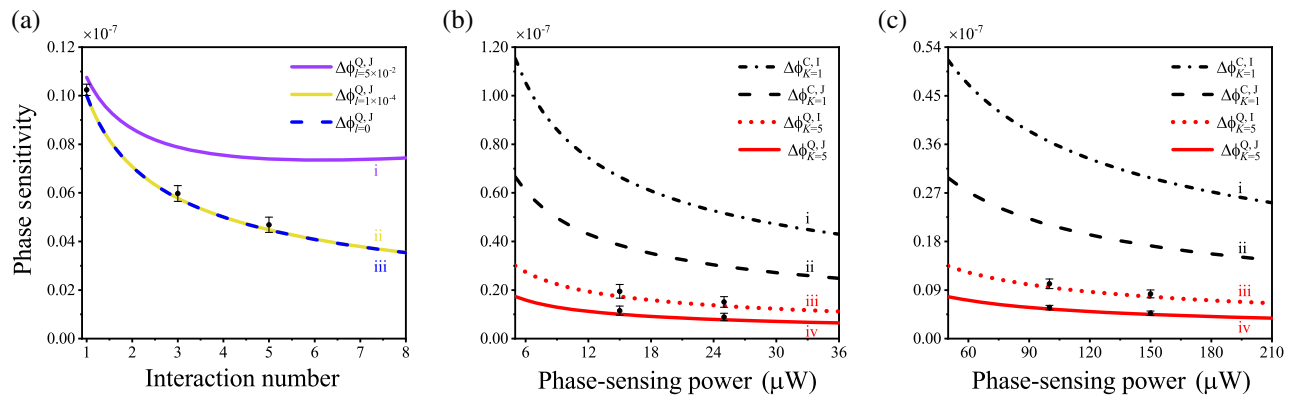


FIG. 3. Experimental results of quantum-enhanced three-arm interferometer. (a) The influence of the interaction number on the joint sensitivity with different mirror losses. The purple solid, yellow solid, and blue dashed traces i, ii, and iii represent the joint sensitivities with mirror losses of 5×10^{-2} , 1×10^{-4} , and lossless, respectively. The points are the experimental results with a mirror loss of 1×10^{-4} . (b),(c) The phase sensitivity for three and two signals versus the phase-sensing power, respectively. The black dotted-dashed and dashed traces i, ii represent the individual and joint sensitivities for the conventional interferometer with single-pass interaction, respectively; and the red dotted and solid traces iii, iv are the individual and joint sensitivities for the quantum interferometer with five-pass interactions, respectively. Error bars representing ± 1 standard error are obtained with the statistics of the measured sensitivity.

signals by employing only the destructive interference output modes measured by BHDs, which overcomes the problem of power saturation at higher phase-sensing powers [68]. (See the Supplemental Material [46] for the experimental details.) Therefore, this combination of parallel and sequential use of squeezing in the interferometer enables high-sensitivity measurements of both joint and individual values for multiple parameters.

In conclusion, we theoretically and experimentally demonstrate how a quantum-enhanced multiarm interferometer efficiently benefits from the parallel and sequential use of squeezed states inside the interferometer. Both joint and individual measurements for multiple signals with high sensitivity are deterministically achieved by amplifying the signals and squeezing the noise simultaneously. And quantum superiority of multiparameter quantum sensing is robust and scalable in this interferometer. Furthermore, our scheme can benefit from the SU(1,1) interferometers to further amplify the signal and counteract the external losses, by replacing the beam splitters in the interferometer with parametric amplifiers. It is possible to construct a larger scale interferometer for quantum-enhanced sensing by merging an integrated photonic platform [69]. The high SNRI at higher frequencies can be realized by employing a broadband quantum source with the high squeezed degree [70]. Notably, the techniques behind these results serve as building blocks for a wide range of high-sensitivity phase dependent devices without disturbing the sample and enable the simultaneous observation of multiple tiny signals merged in quantum noises. This approach paves an attractive avenue for high-speed photoacoustic imaging of living samples, such as blood vessels, with parallel monitoring of multiplexed systems in real time [71]. Our result not only sheds new light on optical high-sensitivity sensing and high-speed imaging in biology and material, but also stimulates further efforts in other applications of quantum interferometer-based array measurements [72].

Acknowledgments—We thank L. Pezzè and A. Smerzi for the helpful discussion. This research was supported by the Innovation Program for Quantum Science and Technology (Grant No. 2024ZD0300900), the Key Project of the National Key R&D program of China (Grant No. 2022YFA1404500), the National Natural Science Foundation of China (Grants No. 61925503, No. 62122044, and No. 62135008), Fundamental Research Program of Shanxi Province (Grant No. 202403021223001), and the fund for Shanxi “1331 Project” Key Subjects Construction.

Data availability—The data that support the findings of this Letter are available from the corresponding authors upon reasonable request.

- [1] C. L. Degen, F. Reinhard, and P. Cappellaro, Quantum sensing, *Rev. Mod. Phys.* **89**, 035002 (2017).
- [2] B. P. Abbott *et al.* (LIGO Scientific Collaboration and Virgo Collaboration), Observation of gravitational waves from a binary black hole merger, *Phys. Rev. Lett.* **116**, 061102 (2016).
- [3] F. Albarelli, M. Mazelanik, M. Lipka, A. Streltsov, M. Parniak, and R. Demkowicz-Dobrzański, Quantum asymmetry and noisy multimode interferometry, *Phys. Rev. Lett.* **128**, 240504 (2022).
- [4] S. Hong, J. u. Rehman, Y.-S. Kim, Y.-W. Cho, S.-W. Lee, H. Jung, S. Moon, S.-W. Han, and H.-T. Lim, Quantum enhanced multiple-phase estimation with multimode NOON states, *Nat. Commun.* **12**, 5211 (2021).
- [5] H.-S. Zhong *et al.*, Quantum computational advantage using photons, *Science* **370**, 1460 (2020).
- [6] J. M. Arrazola *et al.*, Quantum circuits with many photons on a programmable nanophotonic chip, *Nature (London)* **591**, 54 (2021).
- [7] D. J. Bornhop, J. C. Latham, A. Kussrow, D. A. Markov, R. D. Jones, and H. S. Sørensen, Free-solution, label-free molecular interactions studied by back-scattering interferometry, *Science* **317**, 1732 (2007).
- [8] A. Crespi, M. Lobion, J. C. F. Matthews, A. Politi, C. R. Neal, R. Ramponi, R. Osellame, and J. L. O’Brien, Measuring protein concentration with entangled photons, *Appl. Phys. Lett.* **100**, 233704 (2012).
- [9] J. Shi, T. T. W. Wong, Y. He, L. Li, R. Zhang, C. S. Yung, J. Hwang, K. Maslov, and L. V. Wang, High-resolution, high-contrast mid-infrared imaging of fresh biological samples with ultraviolet-localized photoacoustic microscopy, *Nat. Photonics* **13**, 609 (2019).
- [10] C. A. Casacio, L. S. Madsen, A. Terrasson, M. Waleed, K. Barnscheidt, B. Hage, M. A. Taylor, and W. P. Bowen, Quantum-enhanced nonlinear microscopy, *Nature (London)* **594**, 201 (2021).
- [11] C. M. Caves, Quantum-mechanical noise in an interferometer, *Phys. Rev. D* **23**, 1693 (1981).
- [12] R. S. Bondurant and J. H. Shapiro, Squeezed states in phase-sensing interferometers, *Phys. Rev. D* **30**, 2548 (1984).
- [13] V. Giovannetti, S. Lloyd, and L. Maccone, Quantum-enhanced measurements: Beating the standard quantum limit, *Science* **306**, 1330 (2004).
- [14] H. Yonezawa *et al.*, Quantum-enhanced optical-phase tracking, *Science* **337**, 1514 (2012).
- [15] S. Slussarenko, M. M. Weston, H. M. Chrzanowski, L. K. Shalm, V. B. Verma, S. W. Nam, and G. J. Pryde, Unconditional violation of the shot-noise limit in photonic quantum metrology, *Nat. Photonics* **11**, 700 (2017).
- [16] L. Xu, Z. Liu, A. Datta, G. C. Knee, J. S. Lundeen, Y.-q. Lu, and L. Zhang, Approaching quantum-limited metrology with imperfect detectors by using weak-value amplification, *Phys. Rev. Lett.* **125**, 080501 (2020).
- [17] W. Du, J. Kong, G. Bao, P. Yang, J. Jia, S. Ming, C.-H. Yuan, J. F. Chen, Z. Y. Ou, M. W. Mitchell *et al.*, SU(2)-in-SU(1,1) nested interferometer for high sensitivity, loss-tolerant quantum metrology, *Phys. Rev. Lett.* **128**, 033601 (2022).

- [18] T. Nagata, R. Okamoto, J. L. O'Brien, K. Sasaki, and S. Takeuchi, Beating the standard quantum limit with four-entangled photons, *Science* **316**, 726 (2007).
- [19] H. Yu *et al.*, Quantum correlations between light and the kilogram-mass mirrors of LIGO, *Nature (London)* **583**, 43 (2020).
- [20] W. Jia, V. Xu, K. Kuns, M. Nakano, L. Barsotti, M. Evans, N. Mavalvala *et al.*, Squeezing the quantum noise of a gravitational-wave detector below the standard quantum limit, *Science* **385**, 1318 (2024).
- [21] M. Tse, H. Yu, N. Kijbunchoo, A. Fernandez-Galiana, P. Dupej, L. Barsotti, C. D. Blair, D. D. Brown, S. E. Dwyer, A. Effler *et al.*, Quantum-enhanced advanced LIGO detectors in the era of gravitational-wave astronomy, *Phys. Rev. Lett.* **123**, 231107 (2019).
- [22] F. Acernese *et al.* (Virgo Collaboration), Increasing the astrophysical reach of the advanced Virgo detector via the application of squeezed vacuum states of light, *Phys. Rev. Lett.* **123**, 231108 (2019).
- [23] T. J. Proctor, P. A. Knott, and J. A. Dunningham, Multi-parameter estimation in networked quantum sensors, *Phys. Rev. Lett.* **120**, 080501 (2018).
- [24] W. Ge, K. Jacobs, Z. Eldredge, A. V. Gorshkov, and M. Foss-Feig, Distributed quantum metrology with linear networks and separable inputs, *Phys. Rev. Lett.* **121**, 043604 (2018).
- [25] H. Kwon, Y. Lim, L. Jiang, H. Jeong, and C. Oh, Quantum metrological power of continuous-variable quantum networks, *Phys. Rev. Lett.* **128**, 180503 (2022).
- [26] L. Pezzè, M. A. Ciampini, N. Spagnolo, P. C. Humphreys, A. Datta, I. A. Walmsley, M. Barbieri, F. Sciarrino, and A. Smerzi, Optimal measurements for simultaneous quantum estimation of multiple phases, *Phys. Rev. Lett.* **119**, 130504 (2017).
- [27] Z. Hou, J.-F. Tang, H. Chen, H. Yuan, G.-Y. Xiang, C.-F. Li, and G.-C. Guo, Zero-trade-off multiparameter quantum estimation via simultaneously saturating multiple Heisenberg uncertainty relations, *Sci. Adv.* **7**, eabd2986 (2021).
- [28] X.-M. Lu and X. Wang, Incorporating Heisenberg's uncertainty principle into quantum multiparameter estimation, *Phys. Rev. Lett.* **126**, 120503 (2021).
- [29] B. Xia, J. Huang, H. Li, H. Wang, and G. Zeng, Toward incompatible quantum limits on multiparameter estimation, *Nat. Commun.* **14**, 1021 (2023).
- [30] X. Guo, C. R. Breum, J. Borregaard, S. Izumi, M. V. Larsen, T. Gehring, M. Christandl, J. S. Neergaard-Nielsen, and U. L. Andersen, Distributed quantum sensing in a continuous variable entangled network, *Nat. Phys.* **16**, 281 (2020).
- [31] Y. Xia, W. Li, W. Clark, D. Hart, Q. Zhuang, and Z. Zhang, Demonstration of a reconfigurable entangled radio-frequency photonic sensor network, *Phys. Rev. Lett.* **124**, 150502 (2020).
- [32] L.-Z. Liu *et al.*, Distributed quantum phase estimation with entangled photons, *Nat. Photonics* **15**, 137 (2021).
- [33] Y. Xia, A. R. Agrawal, C. M. Pluchar, A. J. Brady, Z. Liu, Q. Zhuang, D. J. Wilson, and Z. Zhang, Entanglement-enhanced optomechanical sensing, *Nat. Photonics* **17**, 470 (2023).
- [34] S. Hong, M. A. Feldman, C. E. Marviny, D. Lee, C. Lee, M. T. Febraro, A. M. Marino, and R. C. Pooser, Quantum enhanced distributed phase sensing with a truncated SU(1,1) interferometer, *Phys. Rev. Res.* **7**, 023231 (2025).
- [35] Y. Zhou, J. Yu, Z. Yan, X. Jia, J. Zhang, C. Xie, and K. Peng, Quantum secret sharing among four players using multipartite bound entanglement of an optical field, *Phys. Rev. Lett.* **121**, 150502 (2018).
- [36] B. K. Malia, Y. Wu, J. Martínez-Rincón, and M. A. Kasevich, Distributed quantum sensing with mode entangled spin-squeezed atomic states, *Nature (London)* **612**, 661 (2022).
- [37] Y. Zhou, W. Wang, T. Song, X. Wang, Q. Zhu, K. Zhang, S. Liu, and J. Jing, Ultra-large-scale deterministic entanglement containing $2 \times 20\,400$ optical modes based on time-delayed quantum interferometer, *Phys. Rev. Lett.* **130**, 060801 (2023).
- [38] R. Nehra, R. Sekine, L. Ledezma, Q. Guo, R. M. Gray, A. Roy, and A. Marandi, Few-cycle vacuum squeezing in nanophotonics, *Science* **377**, 1333 (2022).
- [39] S. Liang, J. Cheng, J. Qin, J. Li, Y. Shi, Z. Yan, X. Jia, C. Xie, and K. Peng, High-speed quantum radio-frequency-over-light communication, *Phys. Rev. Lett.* **132**, 140802 (2024).
- [40] J. A. H. Nielsen, J. S. Neergaard-Nielsen, T. Gehring, and U. L. Andersen, Deterministic quantum phase estimation beyond NOON states, *Phys. Rev. Lett.* **130**, 123603 (2023).
- [41] J. Qin, Y.-H. Deng, H.-S. Zhong, L.-C. Peng, H. Su, Y.-H. Luo, J.-M. Xu, D. Wu, S.-Q. Gong, H.-L. Liu *et al.*, Unconditional and robust quantum metrological advantage beyond NOON states, *Phys. Rev. Lett.* **130**, 070801 (2023).
- [42] X. Zuo, Z. Yan, Y. Feng, J. Ma, X. Jia, C. Xie, and K. Peng, Quantum interferometer combining squeezing and parametric amplification, *Phys. Rev. Lett.* **124**, 173602 (2020).
- [43] F. Hudelist, J. Kong, C. Liu, J. Jing, Z. Y. Ou, and W. Zhang, Quantum metrology with parametric amplifier-based photon correlation interferometers, *Nat. Commun.* **5**, 3049 (2014).
- [44] Y. Levy, Y. Agnon, and H. Azhari, Measurement of speed of sound dispersion in soft tissues using a double frequency continuous wave method, *Ultrasound Med. Biol.* **32**, 1065 (2006).
- [45] V. Giovannetti, S. Lloyd, and L. Maccone, Advances in quantum metrology, *Nat. Photonics* **5**, 222 (2011).
- [46] See Supplemental Material at <http://link.aps.org/supplemental/10.1103/2hsx-5qfr> for additional information about the calculation details and the experimental setup, which includes Refs. [47–65].
- [47] V. Roman-Rodriguez, D. Fainsin, G. L. Zanin, N. Treps, E. Diamanti, and V. Parigi, Multimode squeezed state for reconfigurable quantum networks at telecommunication wavelengths, *Phys. Rev. Res.* **6**, 043113 (2024).
- [48] X. Li, J.-H. Cao, Q. Liu, M. K. Tey, and L. You, Multi-parameter estimation with multimode Ramsey interferometry, *New J. Phys.* **22**, 043005 (2020).
- [49] P. C. Humphreys, M. Barbieri, A. Datta, and I. A. Walmsley, Quantum enhanced multiple phase estimation, *Phys. Rev. Lett.* **111**, 070403 (2013).
- [50] H. A. Bachor and T. C. Ralph, *A Guide to Experiments in Quantum Optics* (Wiley-vch, Weinheim, Berlin, 2004).
- [51] M. Manceau, G. Leuchs, F. Khalili, and M. Chekhova, Detection loss tolerant supersensitive phase measurement

- with an SU(1,1) interferometer, *Phys. Rev. Lett.* **119**, 223604 (2017).
- [52] N. Thomas-Peter, B.J. Smith, A. Datta, L. Zhang, U. Dorner, and I. A. Walmsley, Real-world quantum sensors: Evaluating resources for precision measurement, *Phys. Rev. Lett.* **107**, 113603 (2011).
- [53] J. Yu, Y. Qin, J. Qin, H. Wang, Z. Yan, X. Jia, and K. Peng, Quantum enhanced optical phase estimation with a squeezed thermal state, *Phys. Rev. Appl.* **13**, 024037 (2020).
- [54] D. Li, B. T. Gard, Y. Gao, C.-H. Yuan, W. Zhang, H. Lee, and J. P. Dowling, Phase sensitivity at the Heisenberg limit in an SU(1,1) interferometer via parity detection, *Phys. Rev. A* **94**, 063840 (2016).
- [55] C. Sparaciari, S. Olivares, and M. G. A. Paris, Gaussian-state interferometry with passive and active elements, *Phys. Rev. A* **93**, 023810 (2016).
- [56] H. Vahlbruch, M. Mehmet, K. Danzmann, and R. Schnabel, Detection of 15 dB squeezed states of light and their application for the absolute calibration of photoelectric quantum efficiency, *Phys. Rev. Lett.* **117**, 110801 (2016).
- [57] J. L. Sandell and T. C. Zhu, A review of in-vivo optical properties of human tissues and its impact on PDT, *J. Biophoton.* **4**, 773 (2011).
- [58] A. Kawasaki *et al.*, Real-time observation of picosecond-timescale optical quantum entanglement towards ultrafast quantum information processing, *Nat. Photonics* **19**, 271 (2025).
- [59] P. I. Sund *et al.*, High-speed thin-film lithium niobate quantum processor driven by a solid-state quantum emitter, *Sci. Adv.* **9**, eadg7268 (2023).
- [60] J. Pan *et al.*, Parallel interrogation of the chalcogenide-based micro-ring sensor array for photoacoustic tomography, *Nat. Commun.* **14**, 3250 (2023).
- [61] E. Blomme, D. Bulcaen, and F. Declercq, Air-coupled ultrasonic NDE: Experiments in the frequency range 750 kHz-2 MHz, *NDT&E Int.* **35**, 417 (2002).
- [62] A. Chou *et al.*, Quantum sensors for high energy physics, [arXiv:2311.01930](https://arxiv.org/abs/2311.01930).
- [63] L. S. Madsen *et al.*, Quantum computational advantage with a programmable photonic processor, *Nature (London)* **606**, 75 (2022).
- [64] M. V. Larsen, X. Guo, C. R. Breum, J. S. Neergaard-Nielsen, and U. L. Andersen, Deterministic generation of a two-dimensional cluster state, *Science* **366**, 369 (2019).
- [65] W. Asavanant *et al.*, Generation of time-domain-multiplexed two-dimensional cluster state, *Science* **366**, 373 (2019).
- [66] L. Pezzè and A. Smerzi, Distributed quantum multiparameter estimation with optimal local measurements, [arXiv:2405.18404](https://arxiv.org/abs/2405.18404).
- [67] R. Demkowicz-Dobrzański, J. Kołodyński, and M. Guta, The elusive Heisenberg limit in quantum-enhanced metrology, *Nat. Commun.* **3**, 1063 (2012).
- [68] X. Sun, Y. Wang, L. Tian, S. Shi, Y. Zheng, and K. Peng, Dependence of the squeezing and anti-squeezing factors of bright squeezed light on the seed beam power and pump beam noise, *Opt. Lett.* **44**, 1789 (2019).
- [69] Z. Vernon, N. Quesada, M. Liscidini, B. Morrison, M. Menotti, K. Tan, and J. E. Sipe, Scalable squeezed-light source for continuous-variable quantum sampling, *Phys. Rev. Appl.* **12**, 064024 (2019).
- [70] J. Cheng, S. Liang, J. Qin, J. Li, Z. Yan, X. Jia, C. Xie, and K. Peng, Semi-device-independent quantum random number generator with a broadband squeezed state of light, *npj Quantum Inf.* **10**, 20 (2024).
- [71] H. Jin *et al.*, A flexible optoacoustic blood ‘stethoscope’ for noninvasive multiparametric cardiovascular monitoring, *Nat. Commun.* **14**, 4692 (2023).
- [72] G. Marra *et al.*, Optical interferometry-based array of seafloor environmental sensors using a transoceanic submarine cable, *Science* **376**, 874 (2022).